The Structure of the Atmospheric Boundary Layer in the Central Equatorial Pacific during January and February of FGGE

JAMES K. FIRESTONE

General Software Corporation, Landover, MD 20785 and Laboratory for Atmospheres, NASA/Goddard Space Flight Center, Greenbelt, MD 20771

BRUCE A. ALBRECHT

The Pennsylvania State University, University Park, PA 16802

(Manuscript received 23 September 1985, in final form 4 May 1986)

ABSTRACT

The structure of the atmospheric boundary layer for a region between Hawaii and the equator is studied using dropwindsonde data (~900 soundings) collected in January and February 1979 as part of the First GARP Global Experiment. These data were used to establish the longitudinal and latitudinal variations in the thermodynamic and wind structure of the boundary layer and describe differences in the structure for convectively active and inactive conditions. Low-level inversions (at a pressure of approximately 850 mb) were found to be an important feature of the structure of the boundary layer for undisturbed conditions. Although the frequency of low-level inversions decreased equatorward from Hawaii, the average height of the inversions observed in these regions did not vary significantly in the north–south direction. For convectively undisturbed conditions, low-level inversions are on the average of sufficient strength to suppress deep convection. However, it is shown they could easily be modified by upward vertical motion to give a boundary layer structure similar to that observed in areas where deep convection was observed.

1. Introduction

Our understanding of the tropical atmosphere has been greatly enhanced by a number of field experiments in the last two decades. Although each experiment concentrated on a particular area of the tropics for a limited period of time, the data collected during these experiments provides the basis for much of our description of the tropical atmosphere. These limited datasets are often used to define the mean structure since temporal and spatial variations in the tropics are generally small, except in the vicinity of convective disturbances. In the tropical Pacific our mean description of the structure of the tropical atmosphere is based on data collected during the Line Island Experiment, 1967, (Zipser, 1969) and from radiosonde data from the Marshall Islands collected during the testing of nuclear devices in 1956 (e.g., see the studies of Yanai et al., 1973; Reed and Recker, 1971). These datasets, however, were insufficient for a detailed description of the structure of the boundary layer. Riehl et al. (1951) used data collected from weather ships in the Pacific for a four month period in 1945 to describe downstream variations of the Pacific trades northeast of Hawaii. Neiburger et al. (1961) describe the structure of the atmosphere in the northeastern Pacific and give details of the characteristics of the inversion in this area.

Over the tropical Atlantic, however, there have been a number of studies of the boundary layer for convectively disturbed and undisturbed conditions (Augstein, 1978). Soundings made during the expeditions of the German ship *Meteor* were used to compile statistics on the characteristics of the trade inversion over the Atlantic (Ficker, 1936). The first detailed descriptions of the temperature and moisture structure of the trade-wind boundary layer were made over the Caribbean (Bunker et al., 1948; Malkus, 1958) using aircraft measurements. The structure of the trade-wind boundary layer in the central Atlantic was defined from high resolution radiosonde measurements made during the Atlantic Trade-Wind Boundary Layer Experiment (ATEX), 1969 (Augstein et al., 1973). Radiosonde measurements obtained during the Barbados Oceanographic and Meteorological Experiment (BOMEX), 1969, were used to determine heat and moisture budgets for an undisturbed period over the western Atlantic (Holland and Rasmussen, 1973; Nitta and Esbensen, 1974; Betts, 1975). LeMone and Pennell (1976) used aircraft measurements made in the vicinity of Puerto Rico to study the relationship between trade-wind cumuli and the turbulence structure in the subcloud layer. During the GARP Atlantic Tropical Experiment (GATE), 1974, detailed studies of the structure of the boundary layer were made using tethered balloons and

acoustic sounders (Gaynor and Mandics, 1978; Gaynor and Ropelewski, 1979; Fitzjarrald and Garstang, 1981). The GATE studies have greatly increased our understanding of the interactions between convection and the boundary layer (see review by Houze and Betts, 1981). The time variation of the structure of the boundary layer in the wake of various convective systems was clearly documented during GATE (Houze, 1977; Zipser, 1977; Fitzjarrald and Garstang, 1981; Johnson and Nicholls, 1982). The response of the mixed layer to convective and mesoscale downdrafts during GATE have been modeled by Johnson (1981), Nicholls and Johnson (1984), and Fitzjarrald and Garstang (1981).

Although GATE added greatly to our understanding of the interaction of convection with the boundary layer over tropical oceans, the large-scale flow characteristics in the GATE region are not strictly that of a simple trade-wind flow like that observed in the central Pacific. The circulation is complicated by a monsoonal flow and a low-level easterly jet associated with the north–south surface temperature gradient over the African continent. In addition, some of the convective systems observed in the eastern Atlantic have their origin over Africa. The low-level flow in the central Pacific is very different in that there is no direct continental influence. Another feature of the equatorial central Pacific is the frequent occurrence of a well-defined band of cloudiness associated with the intertropical convergence zone (ITCZ). Consequently, the tropical Pacific north of the equator is a region of transition between the equatorward trade-wind flow and the disturbed convective region of the ITCZ. This transition is not as easily identified in the eastern Atlantic where the trades are modulated by a monsoonal flow near the surface.

The meridional circulation in the eastern and central Pacific is often idealized as an equatorward flow capped by the trade inversion that weakens and increases in height equatorward (e.g., see Schubert, 1976). At the ITCZ the inversion can no longer be maintained and deep convection forms as subsidence gives way to mean upward motion. This is only an average picture, however, since on an individual day the cloudiness associated with the ITCZ may not appear as a well-defined line on satellite imagery, but as individual clusters of cloudiness (Williams and Gray, 1973). However, because this region is basically void of data, the transition between undisturbed and disturbed conditions has not yet been as well documented as it has been in the Atlantic.

In this paper dropwindsonde data (~900 soundings) obtained during the First GARP Global Experiment (FGGE) in 1979 were used to study the structure of the boundary layer for a region between the equator and 15°N and for equatorial regions extending approximately 3000 km both east and west of the longitude of the Hawaiian Islands during January and February. These data are used to define the wind and thermodynamic structure of the boundary layer for a region that has been studied little previously. In addition, satellite photographs are used to categorize soundings as either disturbed or undisturbed to see how the structure of the boundary layer differs with these conditions. These variations in the structure are compared with those observed during GATE to see if the boundary layer characteristics of the GATE area are common to the central Pacific.

2. Description of data

The results described in this paper are based on dropwindsonde data collected during the First Special Observing Period (SOP-1) of FGGE, an international experiment designed to improve our understanding of the atmosphere–ocean system through an extensive set of measurements (Fleming et al., 1979a,b; Smagorinsky, 1978). Although the dropwindsonde measurements were made during FGGE to obtain winds in tropical regions where conventional measurements were not available, they also provided high vertical resolution (~4 mb) thermodynamic soundings. A detailed description of the dropwindsonde programs during FGGE is given by Julian (1982). In this study soundings collected between 15 January and 20 February 1979 from U.S. Air Force C-141 flights between Hawaii and the equator were analyzed. Typically, two flights were made daily along the average flight paths shown in Fig. 1. On any given day, the patterns often deviated from the average by as much as 1–2° latitude or longitude in order to avoid intense convection or the paths of FGGE ships collecting upper-air data. The sondes were dropped from a 13 km altitude (so that they could start transmitting at a pressure of approximately 200 mb). Drops were made approximately every 350 km along the flight path. Soundings were classified according to their geographical location within the four regions shown in Fig. 1. Regions II and III were used to study north–south variations at the southern limit of the trades, and regions I and IV, which parallel the equator, were used to study east–west variations.

The temperature, dewpoint and wind data from the dropwindsondes were analyzed between 600 and 1000 mb. The data obtained for ten second intervals (the

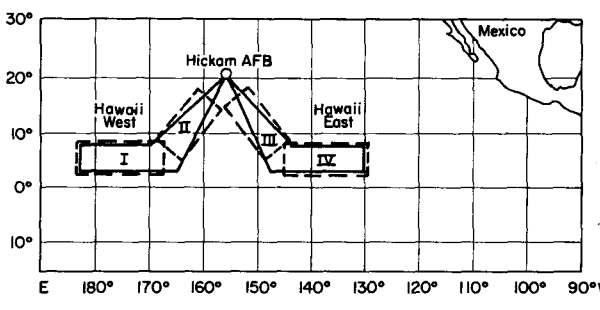

FIG. 1. Approximate flight paths flown during FGGE SOP-1 dropwindsonde missions in the Pacific. The soundings were analyzed based on their location within the four rectangular areas (I–IV) shown.

dropsonde fall rate is ~25 mb min^{-1}) during descent were smoothed using a 1–2–1 smoother and interpolated to 10 mb levels. These data were then used to calculate potential temperature θ, mixing ratio q, equivalent potential temperature θ_e, and saturation equivalent potential temperature θ_{es}. The mixing ratio and potential temperature profiles for each sounding were plotted and questionable data were identified by subjectively screening each sounding for unrealistic values or unrealistic vertical gradients. Approximately 10% of the original 900° thermodynamic soundings were found to have either missing or questionable data. The dropwindsonde winds were obtained using an Omega wind-finding system (Julian, 1982). The vertical resolution of the winds is significantly less than that of the thermodynamic data and are considered to be accurate to within 2 m s^{-1} for a pressure interval of ~100 mb.

In addition to the dropwindsonde data, GOES infrared satellite photographs were used to classify the convective activity in the vicinity of each sounding as either disturbed or undisturbed. Winds obtained from the ECMWF FGGE gridded data (Bengtsson et al., 1982) were used to calculate divergence and mean vertical velocity for the region of interest.

3. Regional variations

The soundings were sorted based on their location within the four regions shown in Fig. 1. to allow for a comparison of regional differences in the structure of the boundary layer. The average profiles of potential temperature and mixing ratio for the four regions are shown in Figs. 2 and 3. The variations in potential temperature at the surface reflect sea surface temperature differences among the three regions. Sea surface temperatures are highest in the equatorial regions and increase from east to west. The westernmost region (Region I) is approximately 1.5°C warmer near the surface than the equatorial region east of Hawaii (Region IV). The potential temperature differences at 600 mb are smaller than the variations near the surface, although the more northerly regions (II and III) remain slightly colder than the equatorial regions (I and IV) at this level.

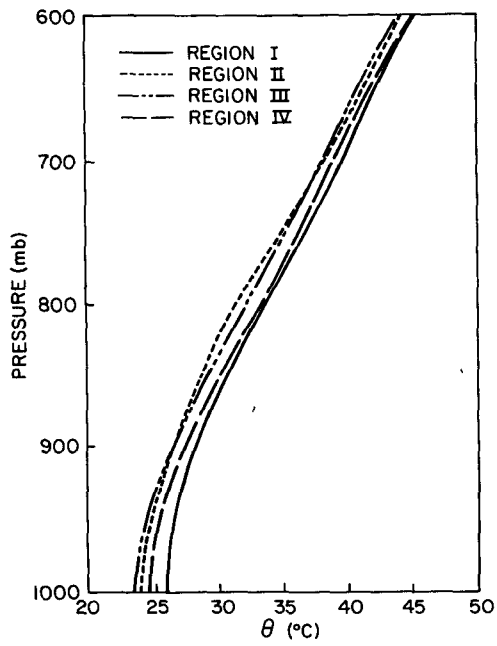

FIG. 2. Mean potential temperature profiles for the four regions shown in Fig. 1.

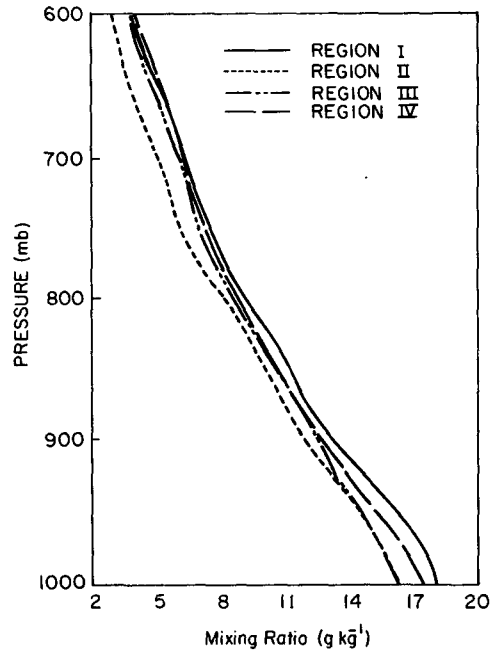

FIG. 3. As in Fig. 2 but for mixing ratio.

Although the averaging tends to smooth the profiles, some structure remains in the mean soundings. The vertical gradient of potential temperature between 950 and 1000 mb is relatively small—consistent with the mixed-layer assumption that is often made in modeling the subcloud layer in regions of convection (e.g., Arakawa and Schubert, 1974; Albrecht et al., 1979). There is, however, a decrease in the mixing ratio with height in the lowest layers in all four regions, which is similar to the decrease observed over land (Mahrt, 1976) and in other tropical regions (e.g., Fitzjarrald and Garstang, 1981). The mixing ratio in the layer between 800 and 600 mb is approximately the same for regions I, III and IV. This layer, however, is drier in region II than the other regions. This dry region may be due to the intrusion of dry air from higher latitudes that is associated with the northerly flow behind midlatitude fronts that penetrate anomalously far south in the winter of 1978–79 (Wagner, 1979). Further evidence for this is shown in the wind profiles later in this section.

The potential temperature profiles for all four regions

show a slightly more stable layer around 800 mb. This layer is due to low-level inversions (defined as a sharp increase in potential temperature through at least a 20 mb depth, between 600 and 900 mb) in a number of the soundings and is more clearly defined in the profiles of saturation equivalent potential temperature shown in Fig. 4. Conditional instability is indicated by a decrease in θ_{es} with height. The stable layer near 800 mb is the only layer below 600 mb that is not conditionally unstable. It will be shown that for undisturbed conditions, the low-level inversions responsible for the stable layer in the mean soundings are of sufficient strength to inhibit convective activity. The profiles of θ_e in Fig. 5 show a layer of potential instability ($\partial\theta_e/\partial z < 0$) extending from 1000 to 750 mb. The minimum in θ_e is consistent with that observed for other tropical regions, although for the FGGE soundings θ_e is approximately constant from 750 to 600 mb. The differences in θ_e for the four regions primarily reflect variations in the mixing ratio.

North–south and east–west variations were obtained by constructing cross sections along the major axis of the four rectangular areas defined in Fig. 1. This was done by dividing each area equally into five rectangular areas. Soundings falling within these smaller areas were averaged to give sections along the major axis of the four areas labeled I–IV in Fig. 1. Areas II and III were used to define north–south variations. Since these areas do not have a strict north–south orientation, variations along these sections will also represent variations in the east–west direction. However, the east–west difference between region II and III and those between I and IV were found to be relatively small.

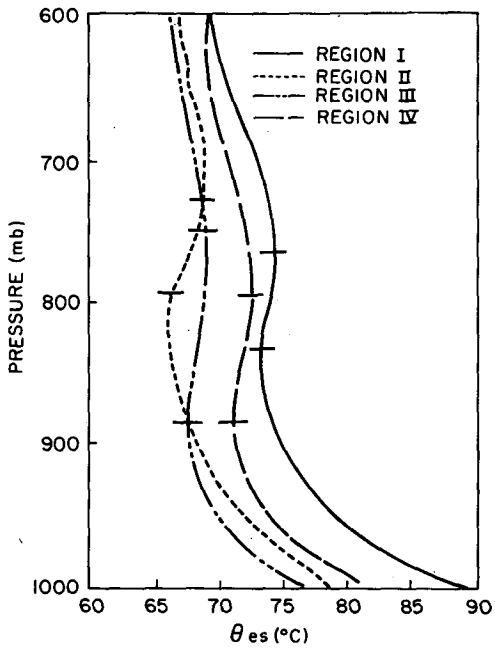

FIG. 4. As in Fig. 2 but for saturation equivalent potential temperature. Thin horizontal lines indicate top and bottom of the stable layer in each average sounding.

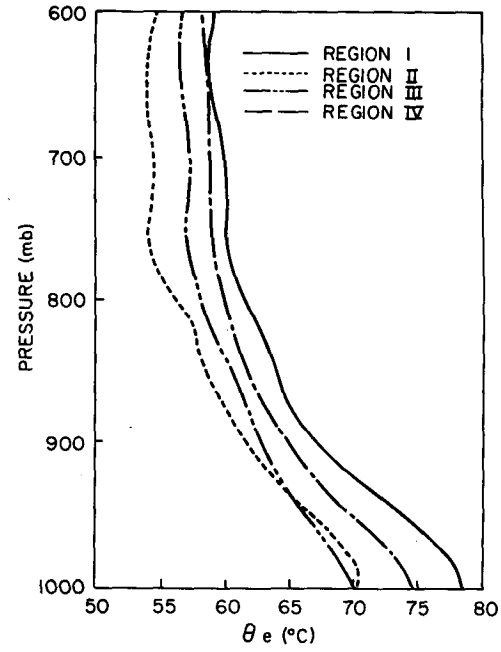

FIG. 5. As in Fig. 2 but for equivalent potential temperature.

The north–south variations in the thermodynamic structure are shown for region II in Figs. 6–9. Only region II will be shown here since region III exhibited similar north–south variations. The variation of potential temperature in region II (Fig. 6) shows relatively little north–south temperature gradient at 600 mb compared with the gradient near the surface, which is about 2°C for 8° latitude. This results in a destabilization of the boundary layer as the air flows southward. The equivalent section of mixing ratio (Fig. 7), shows a significant southward moistening near the surface between 15° and 7°N (from 14.5 to 18.0 g kg^{-1}) with relatively little variation in mixing ratio at 600 mb.

The north–south variations of temperature and moisture near the surface result in a variation of θ_e at the surface of 14°C between 7° and 15°N (Fig. 8). The corresponding difference at 600 mb is only 8°C. The mean cross section of equivalent potential temperature shows little vertical variation about 750 mb, although there is a well-defined minimum just below this level. The minimum θ_e shown in Fig. 8 is located *above* the inversion and is due to relatively dry air that is present at all latitudes.

The north–south cross section of saturation equivalent potential temperature (Fig. 9) clearly shows that the layer near 750 mb is stable. This stable layer results from low-level inversions, which are present in many of the soundings. The θ_{es} cross section shows that there is no appreciable increase in the height of the inversions

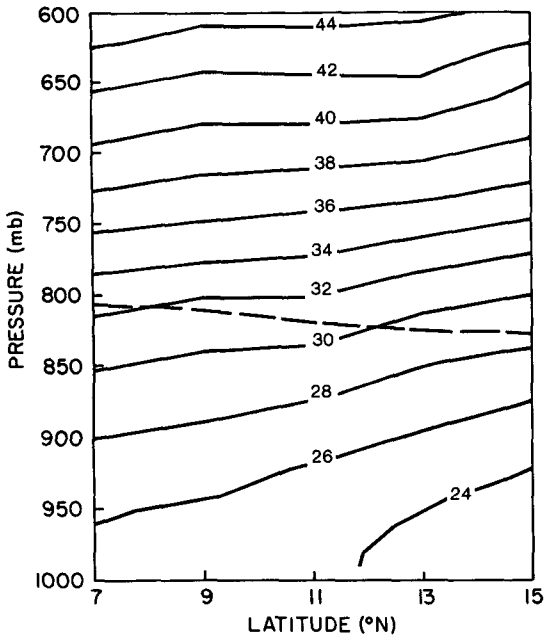

FIG. 6. Region II mean cross section of potential temperature. Dotted line indicates mean inversion base determined from θ_{es} cross sections.

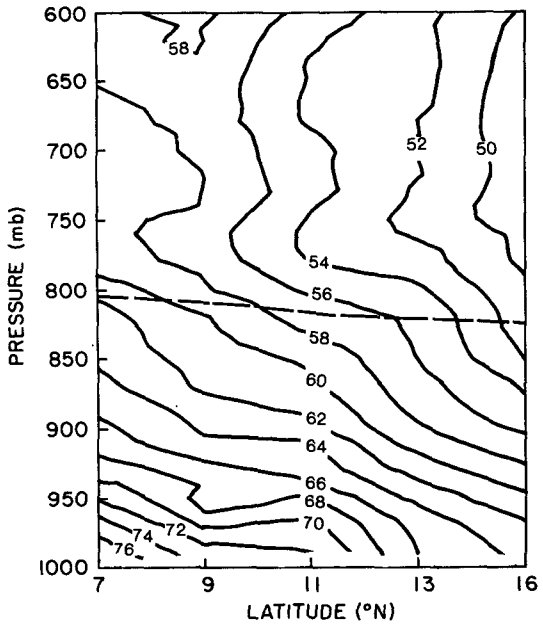

FIG. 8. As in Fig. 6 but for equivalent potential temperature.

toward the equator, as is often assumed in the idealized equatorward flow associated with the Hadley circulation. The inversion height shown in Figs. 6–9 is based on the θ_{es} minimum for the average cross section and not the individual soundings.

Since subsidence is important in determining the height of low-level inversions (Albrecht et al., 1979), these results might indicate that where low-level inversions are observed near 7°N the subsidence may be as strong as it is at 15°N. However, during the period when the dropwindsonde measurements are made, the

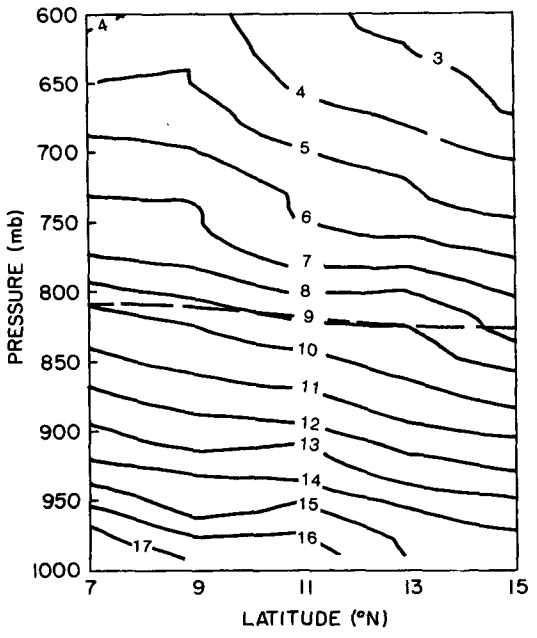

FIG. 7. As in Fig. 6 but for mixing ratio.

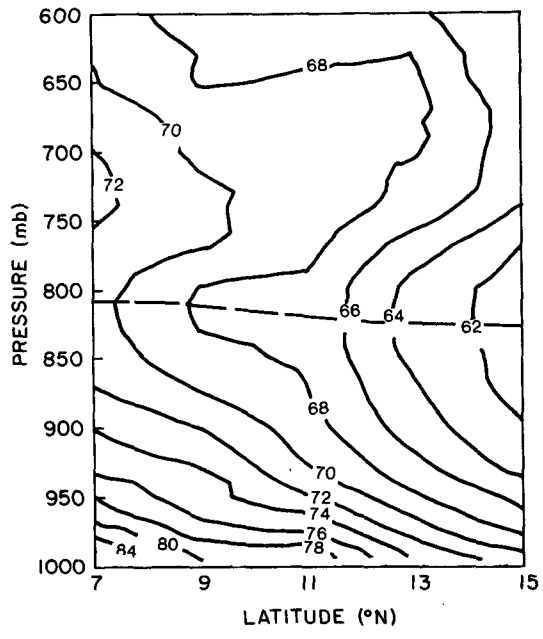

FIG. 9. As in Fig. 6 but for saturation equivalent potential temperature.

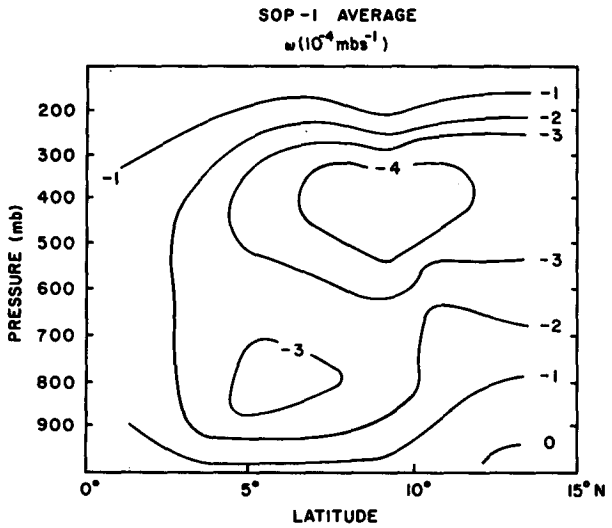

FIG. 10. Mean vertical velocity ω calculated from ECMWF winds. Values are averaged longitudinally from 135° to 175°W and are for SOP-1 (after Felde, 1983).

mean vertical motion in the region of interest is upward. This is shown in Fig. 10 where the mean vertical velocity obtained from the ECMWF winds (using the kinematic method and a mass balance correction) is shown for a north–south section calculated for the period 15 January to 15 February 1979 and averaged between 135° and 175°W. At 750 mb the upward vertical velocity increases southward to a maximum near 6°N. The soundings with low-level inversions, however, were generally obtained in regions of suppressed convection and may have been maintained by subsidence associated with deep convection. Thus, despite the increase in the large-scale upward motion equatorward, compensating subsidence in regions surrounding deep convection may help maintain relatively low-level stable layers, which in turn inhibit the convective activity. Although the mean height of the inversion does not vary significantly in the north–south direction, the frequency of occurrence of deep convective activity increases and the frequency of occurrence of low-level inversions decreases southward (see section 4). Thus, the subsidence in suppressed regions near the equator may be as large as it is in the subtropics, but the total area affected by subsidence decreases downstream.

East–west cross sections were obtained for regions I and IV. These cross sections revealed very little structure in the east–west direction and are not presented here. The east–west variation is best shown by the mean differences between region I and IV illustrated in Figs. 2–5. The differences in potential temperatures between regions I and IV would indicate a sea surface temperature difference of about 1.5°C and a corresponding difference in mixing ratio near the surface of 1.5 g kg^{-1}. In section 4, statistics based on satellite imagery show that region I is the most convective region of the four analyzed. An analysis of the vertical velocity obtained from the ECMWF winds also indicate that the mean upward motion in region I was approximately twice that observed in region IV (Firestone, 1983).

Average profiles of the zonal and meridional components of the wind are shown in Figs. 11 and 12. Since the wind data from the dropwindsondes are only reliable for layers of approximately 100 mb thick, the profiles presented were smoothed to remove small-scale variations. These profiles show that all four regions

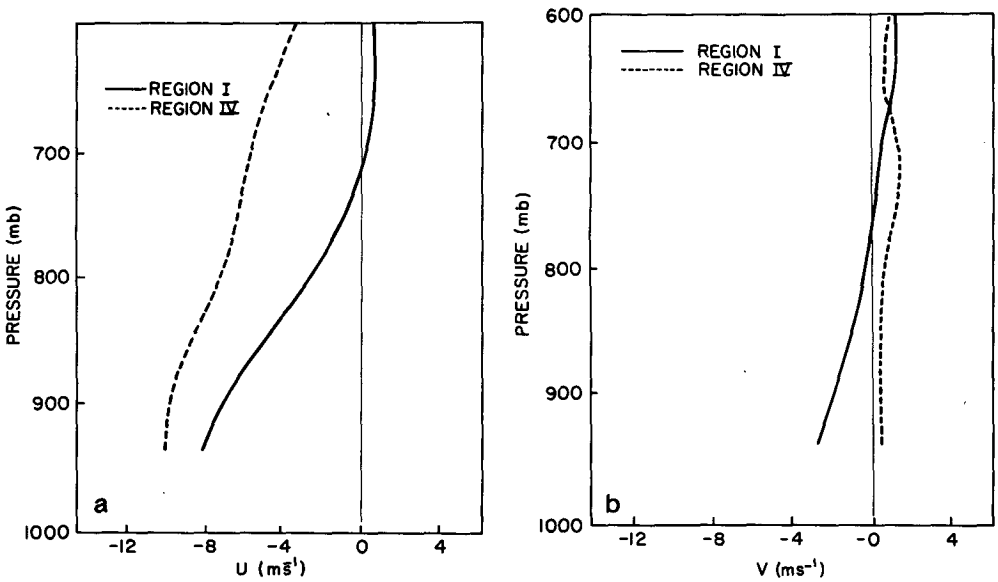

FIG. 11. (a) Mean zonal component u of the wind for equatorial regions (I and IV), and (b) mean meridional component v.

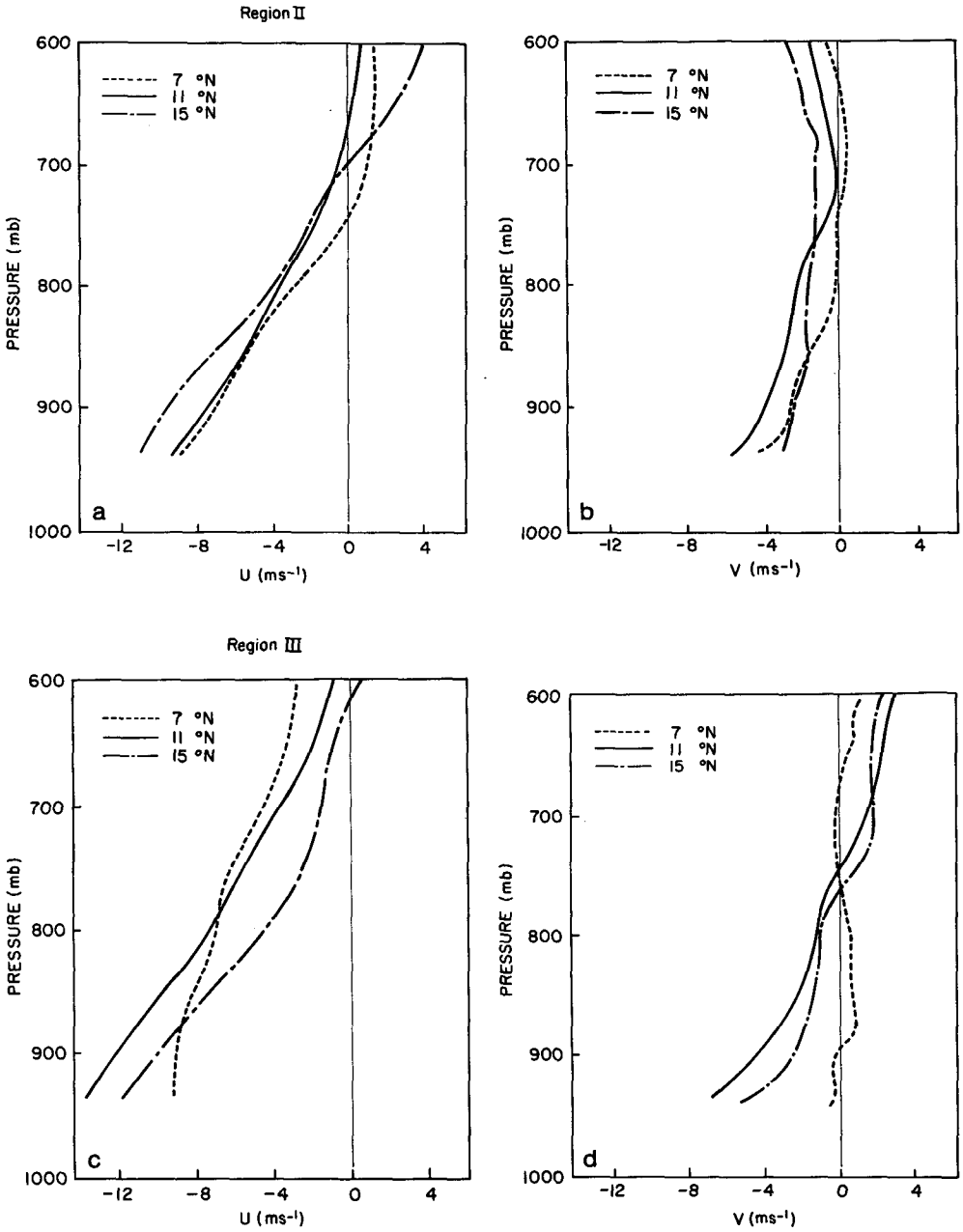

FIG. 12. (a) Mean zonal component u of the wind for region II at different latitudes, (b) mean meridional component v, (c) zonal component for region III, and (d) meridional component.

were dominated by easterly flow near the surface that weakens with height, consistent with the northward decrease in temperature. In the northern parts of region II the winds become westerly above 700 mb, consistent with the possible influence of midlatitude frontal systems in this region (Wagner, 1979). The slightly greater vertical shear in the zonal component in region II implies a greater north–south temperature gradient than in region III. Between 7° and 15°N at 850 mb the temperature differences in regions II and III were 3° and 2°C, respectively.

The meridional component of the wind is from the north near the surface in all the regions except region IV. Here the winds are weak and from the south. This region appears in the mean to be slightly south of the ITCZ. The corresponding region to the west of Hawaii (Region I) appears to be slightly north of the ITCZ with northerly winds at the surface. This region is,

however, more active convectively than region IV. The northerly winds tend to weaken with height in the three regions (Regions I, II and III) to a minimum near 700 mb with southerlies about this level. These findings are consistent with those of Ramage et al. (1979) and Riehl (1979) where it was suggested that the above-inversion air north of the equator originates in the Southern Hemisphere.

The wind profiles shown here are similar to those observed during ATEX with maximum easterlies and notherlies at about 950 mb and with the easterlies confined to the lowest 150–200 mb. The FGGE winds, however, are stronger than those observed in the Atlantic during ATEX, possibly due to the anomalously strong subtropical Pacific high in early 1979. Although the climatology given by Newell et al. (1972) shows easterlies extending through a greater depth of the atmosphere (to about 500 mb) than for the results here, it does show a maximum in the low-level easterlies in the December–February average at a longitude of 170°W at 10°N.

4. Variations of boundary layer structure with convective activity

The soundings obtained within the four regions discussed were further categorized as disturbed or undisturbed based on the GOES-West infrared satellite photos. Drops made in areas completely covered by high cloud tops were classified as disturbed. In a few cases where this classification was ambiguous, the classification of disturbed or undisturbed was based on the sounding, since in the remainder of the soundings there was a high degree of correlation between undisturbed conditions and the presence of an inversion, and disturbed conditions with no inversion (see Fig. 14). Thus, if the satellite photo gave an ambiguous classification but an inversion was present, the sounding was classified as undisturbed. Overall, 52% of the 867 soundings analyzed for the four regions were classified as undisturbed.

Figure 13 illustrates how the frequency of undisturbed conditions varies with latitude. This figure was constructed by averaging regions II and III together for latitudes between 7° and 15°N and averaging regions III and IV to represent values at 5°N. There is a slight decrease in undisturbed conditions equatorward, with a minimum in undisturbed conditions at approximately 9°N. In addition, the equatorial region located to the west of Hawaii (I) was found to be more convectively active than the corresponding region east of Hawaii (IV). In region I, 41% of the soundings were undisturbed, and in region IV 66% of the soundings were undisturbed. Within regions I and IV there is an increase in disturbed conditions from east to west. The statistics on convective conditions may be slightly biased, however, since the flights were flown on a path that would avoid the deepest convection and there may be more data rejected from soundings dropped in regions of convective activity.

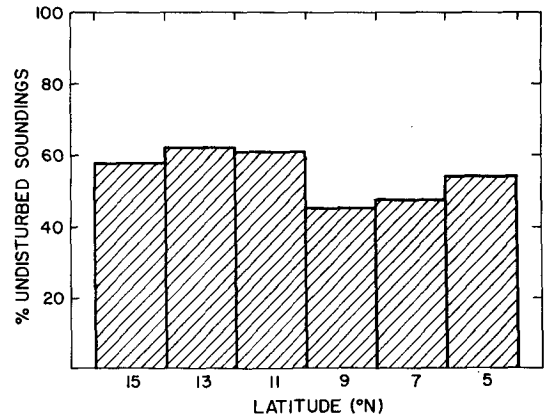

FIG. 13. Percentage of all soundings classified as undisturbed as a function of latitude for the four regions.

Although the subjective classification scheme used can only be considered a crude measure of convective activity, it is consistent with the satellite classification used by Williams and Gray (1973) in their study of tropical cloud clusters. Furthermore, Thompson et al. (1979) found good correspondence between convective cloudiness estimated from satellite photographs and precipitation rates for different regions within easterly wave systems observed during GATE.

The soundings were examined subjectively for the presence of low-level inversions. Figure 14 shows the percentage of undisturbed soundings with inversions (unshaded portion) and the percentage of all soundings with inversions (shaded portions). Although there is clearly a decrease in the number of soundings with inversions equatorward, it is clear that low-level inversions are a prevalent feature of the equatorial boundary layer during the period analyzed. At 5°N over 50% of the soundings had low-level inversions.

Differences between the thermodynamic structure observed for disturbed and undisturbed conditions were examined for regions I and IV. These regions were chosen since there was relatively little variation of sea surface temperature between them to complicate the comparison. The mean potential temperature and mixing ratio profiles for the disturbed and undisturbed soundings in region I are shown in Fig. 15. The disturbed soundings are warmer in the layer between 950 and 825 mb than the undisturbed soundings, and cooler in the layer above. The disturbed soundings are clearly more moist than the undisturbed soundings for this region at all levels. During GATE it was found that for disturbed conditions the boundary layer tended to be cooler and drier (particularly within the lowest 500 m) than for undisturbed conditions in regions influenced by downdrafts. It was observed that it would sometimes take several hours for the boundary layer to recover from the disturbed state (Zipser, 1977; Fitz-

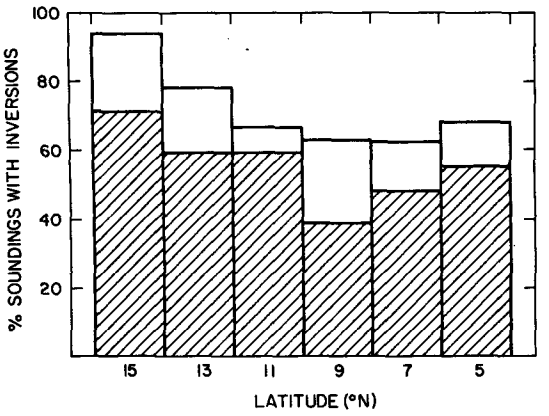

FIG. 14. Percent of undisturbed soundings with low-level inversions and percent of all soundings (shaded areas) with inversions.

jarrald and Garstang, 1981). The disturbed mean profiles shown in Fig. 15a probably contain soundings that were obtained in regions of boundary layer air that had been modified by downdrafts, even though the average profiles do not reflect these features. Firestone (1983), for example, showed soundings obtained in the vicinity of a well-defined convective system that had apparently been modified by downdrafts. The differences between the average temperature and moisture structure for disturbed and undisturbed conditions in region IV (not shown here) were similar to those obtained for region I.

Although the mean disturbed profile differs only slightly from the undisturbed, there are important differences in the stability of the lowest layer. This is illustrated in Fig. 16 where θ_e and θ_{es} for the disturbed and undisturbed conditions in region I are shown. An important feature of these profiles is the stable layer near 800 mb shown by the mean θ_{es} profile for the undisturbed case. The θ_e path for a nonentraining parcel originating from 975 mb is shown. Above the lifting condensation level (LCL) the difference between this path and the θ_{es} profile will be proportional to the temperature difference between a parcel originating from 975 mb and the temperature of the environment. For the mean disturbed sounding for region I there would be sufficient buoyancy to support convection to at least 600 mb. For the undisturbed sounding a nonentraining parcel would need a θ_e from 975 mb or a higher pressure to support deep convection. The ascent of an entraining parcel would clearly be inhibited by the stable layer at 800 mb. The presence of some soundings classified as disturbed but with weak inversions results in a slightly stable layer near 800 mb for the disturbed soundings shown in Fig. 16b.

The low-level stability associated with the disturbed and undisturbed soundings in region IV show similar features (Fig. 17), although the inversion layer in this case is more stable than for the mean undisturbed sounding in region I. In this region even a nonentraining parcel originating from 975 mb would be unable to penetrate the stable layer present in the mean undisturbed sounding. For the mean disturbed profile for region IV there is evidence of a stable layer at 750 mb, but it is insufficient to inhibit deep convection. The relatively high stability of the mean undisturbed profile of region IV is consistent with the observation of relatively little convection as shown by the GOES imagery.

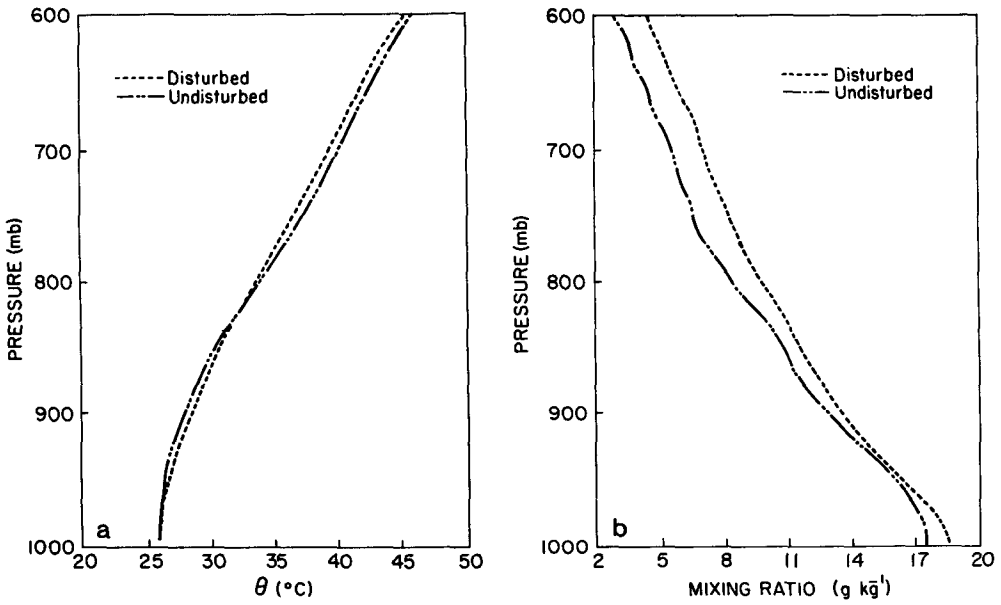

FIG. 15. Comparison of the (a) potential temperature and (b) mixing ratio for disturbed and undisturbed conditions in region I.

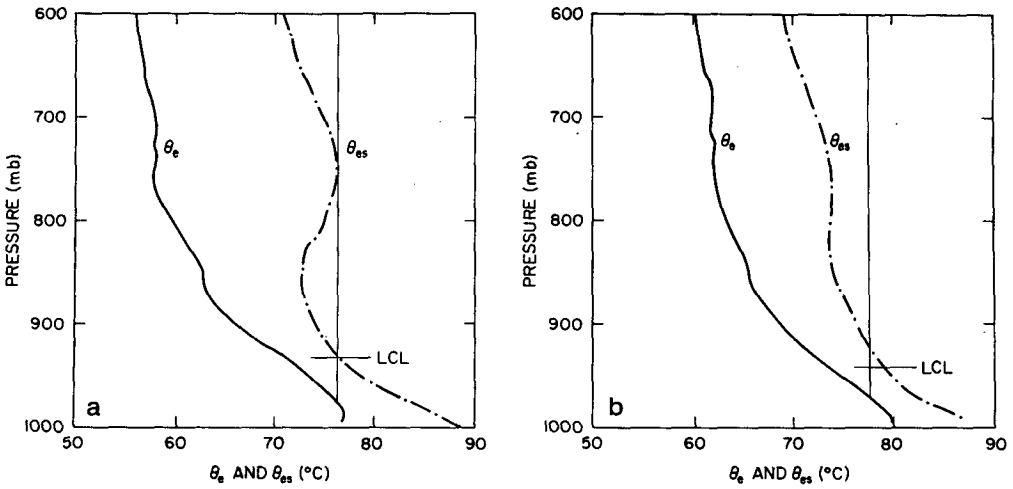

FIG. 16. (a) Average θ_e and θ_{es} profiles for the undisturbed soundings of region I and (b) the disturbed soundings in region I. The thin line indicates θ_e for a parcel originating at 975 mb. The lifting condensation level (LCL) of this parcel is also indicated.

The presence of low-level inversions in the mean undisturbed sounding for region I is further illustrated by noting the large variance in potential temperature near 800 mb (Fig. 18). There is no maximum in the variance at this level for the disturbed soundings. The variability in the undisturbed soundings is due to changes in height of the inversions in time and space, although the structure above and below the inversions remains fairly constant.

Low-level inversions observed near the equator are clearly of sufficient strength to inhibit deep convection. They may be maintained by subsidence induced by nearby deep convection or by mean large-scale subsidence. If they are maintained by convectively induced subsidence, this would provide a mechanism to help maintain the organization of convective systems by suppressing deep convection in the regions surroundings these systems. Likewise, upward vertical motion in the vicinity of these systems would weaken the inversions and allow the formation of deep convection.

Although upward vertical velocity in the boundary layer has long been recognized as a condition for the formation of deep convection, the exact mechanism responsible for the positive correlation between low-level convergence and deep convection has not always been made clear. To illustrate how upward motion in the boundary layer can weaken low-level inversions, a simple calculation was made starting from the undisturbed θ profile for region IV. A simple time-stepping procedure was used to calculate the time variation of θ due to vertical advection $[-\omega(\partial\theta/\partial p)]$. The modified θ_{es} profile was then obtained from the calculated θ val-

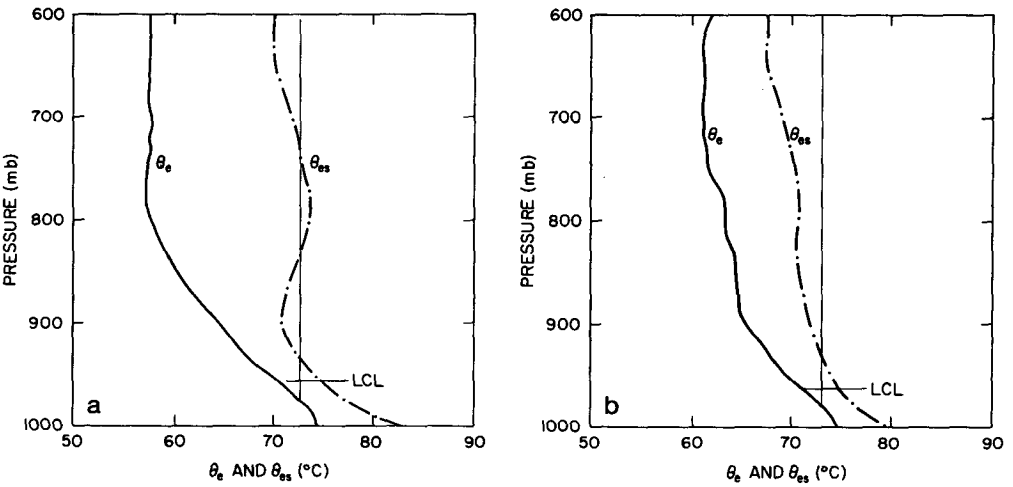

FIG. 17. As in Fig. 16 but for region IV.

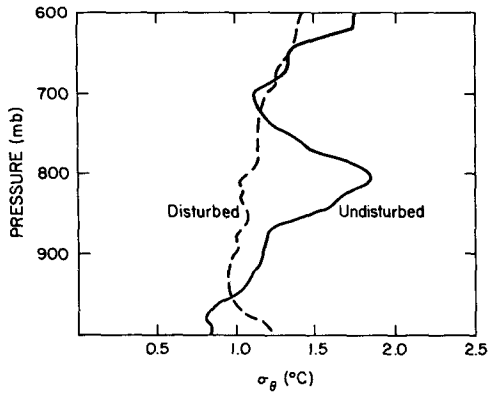

FIG. 18. Standard deviation of potential temperature for Region I for disturbed and undisturbed soundings.

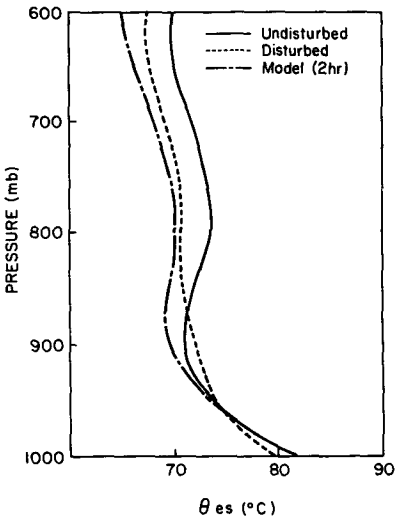

FIG. 19. The mean profile of θ_{es} for the undisturbed soundings in region IV, the θ_{es} profile that would result if the mean sounding were modified by the upward motion associated with a mean divergence of (1×10^{-5} s^{-1}) for 120 minutes, and the mean profile of θ_{es} for disturbed conditions in region IV.

ues. The vertical velocity for this calculation was assumed to vary linearly with height by assuming a convergence of 1×10^{-5} s^{-1} that was independent of height. The effect of vertical advection on the low-level stability is illustrated in Fig. 19, where the solution after 2 is shown. The stretching of the layer by vertical advection has almost completely removed the conditional stability at 800 mb in two hours. The mean height of the stable layer, however, has not changed significantly (about 10 mb) in this time. The modified profile would support deep convection and is similar to the profile of θ_{es} observed for the disturbed case, which is also shown in Fig. 19. Other processes may also be responsible for the transition between the undisturbed and disturbed profiles since vertical advection cannot explain the warming at 900 mb that would be needed to duplicate the change between the undisturbed and disturbed profiles. For instance, mesoscale downdrafts could adiabatically warm air in the lower levels. The magnitude of upward motion assumed in this calculation would correspond to that associated with large-scale circulations and would suggest a lag between the upward vertical motion and deep convection. The convergence value chosen here was arbitrary. For other values of convergence, the time required to obtain the same amount of modification as shown in Fig. 19 could be estimated by scaling the convergence to the 1×10^{-5} s^{-1} value. For example, the convergence associated with a squall line might easily be an order of magnitude larger than the convergence assumed in this simple calculation. Consequently, for a squall line the time required to destabilize the boundary layer would be an order of magnitude less than that calculated here.

Studies of the structure of the boundary layer during GATE concentrated on its recovery after it was modified by meso- and convective-scale downdrafts (e.g., Fitzjarrald and Garstang, 1981; Johnson and Nicholls, 1982). It has been estimated that the GATE area was under the influence of wake regions for about 30% of the time (Gaynor and Mandics, 1978). The modification of the boundary layer in the wake of squall systems was studied in detail during GATE. Although the stable layer at cloud base was a focus of much of the GATE research (e.g., Nicholls and Johnson, 1984), the role of inversions at the top of a shallow cloud layer was not considered in detail. In the region being studied here, it is apparent that low-level inversions are important for regulating deep convection, since the temperature and moisture in the boundary layer for this case did not differ significantly between disturbed and undisturbed conditions.

Although the role of downdrafts on boundary layer structure was not totally assessed in this study, individual soundings do show evidence of boundary layer modification by downdrafts (Firestone, 1983) that is consistent with the modification observed during GATE. One would expect downdraft events to be signified by variations in θ_e of the low levels of the atmosphere (Barnes and Garstang, 1982). However, the standard deviation of θ_e was found to be about the same for both the disturbed and the undisturbed soundings in both regions I and IV (See Table 1). The

TABLE 1. Standard deviation of θ_e for disturbed (D) and undisturbed (UD) conditions in region I and IV (Units: K).

Pressure (mb)	Region I		Region IV	
	D	UD	D	UD
980	5.4	5.8	5.2	4.4
960	5.0	5.2	5.3	4.7
940	5.2	5.2	5.8	5.0

average standard deviation of θ_e is about 5°C. The standard deviation of potential temperature for these cases is about 1°C. If some of the observed variance is due to modification by downdrafts, either downdraft events are included in with both the disturbed and the undisturbed soundings or other processes (including possibly instrument error) are primarily responsible for the variance in θ_e.

5. Summary

Dropwindsonde data collected during FGGE were used to establish the mean structure of the atmospheric boundary layer for January and February of 1979 in the central equatorial Pacific. The north–south variation in the thermal structure showed a destabilization of the boundary layer equatorward due to an equatorward increase in the temperatures near the surface and very little change in the temperature at 600 mb. The mean soundings at all latitudes had a conditionally stable layer near 800 mb (saturation equivalent potential temperature increasing with height). There was little evidence to support the idea that the height of the inversion significantly increases toward the equator in this region of the tropics. This observation is consistent with the aircraft measurements described by Ramage et al. (1979). Deep convective activity, as deduced from GOES satellite photographs, increased equatorward to a maximum near 7°N and the frequency of occurrence of low-level inversions also decreases, although over 50% of the soundings obtained near the equator had low-level inversions. At all latitudes the equivalent potential temperature between 750 and 600 mb was found to be nearly constant with height.

The east–west differences were studied using two regions centered at about 5°N—one located between 165° and 185°W and the other from 130° to 145°W. The western region was found to be slightly warmer in the low levels than the eastern region with relatively little difference near 600 mb. In addition, the western region had significantly more deep convective activity than the corresponding region to the east.

All the regions studied were characterized by easterly flow in the low levels that decreased in intensity with height and by northerly flow that also decreased in strength with height. Near 600 mb the meridional flow was from the south, indicating the possibility of cross equatorial flow in these regions.

Mean soundings obtained in regions of deep convection were compared with those obtained for relatively suppressed convective activity. Inversions were shown to result in a sufficiently stable layer in the lower levels of the atmosphere to suppress convection. A simple calculation illustrated how vertical advection could destabilize the boundary layer sufficiently to allow for the development of deep convection. This destabilization occurs by vertical stretching of the inversion layer and not through the deepening of the boundary layer. The inversions observed in this area of the tropics appear to be an important mechanism for regulating deep convection. The convective classification scheme used here did not allow for determination of how convective activity may have been influenced by downdrafts. Thus, in this study it was not possible to exactly compare the results of this study with the GATE findings that showed the boundary layer structure to be significantly modulated by convective and mesoscale downdrafts.

Although the classification of soundings based on the satellite images is relatively crude, the average thermodynamic structures obtained from this classification show significant differences in the stability of the lower troposphere. This suggests that the low-level stability may provide a useful means for classifying the soundings for different convective states. For soundings with low-level inversions, compositing relative to the height of the inversion would help preserve vertical gradients of the various thermodynamic quantities (Augstein et al., 1974).

This analysis indicates the basic utility of the FGGE Pacific dropwindsonde data for describing the structure of the boundary layer in a region where there have been few observations. The analysis is presently being extended to include the SOP-2 soundings and will be used to determine seasonal variations in the boundary layer structure and to understand the transitions between different convective states. In addition, the climatology presented in this paper should be useful for evaluating how well the data assimilation schemes used to produce the gridded FGGE data are able to capture the important features of the tropical boundary layer.

Acknowledgments. We would like to thank Dr. Paul Julian for kindly supplying us with the data used in this study. This research was supported jointly by the National Science Foundation and the National Oceanographic and Atmospheric Administration under grants ATM 83-10434 and ATM 80-09307.

REFERENCES

Albrecht, B. A., 1979: A model for the thermodynamic structure of the trade-wind boundary layer. II: Applications. *J. Atmos. Sci.*, **36**, 90–98.

——, A. K. Betts, W. H. Schubert and S. K. Cox, 1979: A model of the thermodynamic structure of the trade-wind boundary layer. Part I: Theoretical formulation and sensitivity tests. *J. Atmos. Sci.*, **36**, 73–89.

Arakawa, A., and W. H. Schubert, 1974: Interaction of a cumulus cloud ensemble with the large-scale environment, Part I. *J. Atmos. Sci.*, **31**, 674–701.

Augstein, E., 1978: The atmospheric boundary layer over the tropical oceans. *Meteorology Over the Tropical Oceans,* Roy. Meteor. Soc., 73–103.

——, H. Riehl, F. Ostapoff and V. Wagner, 1973: Mass and energy transports in an undisturbed Atlantic trade-wind flow. *Mon. Wea. Rev.*, **101**, 101–111.

——, H. Schmidt and F. Ostapoff, 1974: The vertical structure of the atmospheric planetary boundary layer in undisturbed trade

winds over the Atlantic Ocean. *Bound.-Layer Meteor.*, **6**, 129–150.

Barnes, G., and M. Garstang, 1982: Subcloud layer energetics of precipitating convection. *Mon. Wea. Rev.*, **110**, 102–117.

Bengtsson, L., M. Kanamitsu, P. Kallberg and S. Uppala, 1982: FGGE four dimensional data assimilation at ECMWF. *Bull. Amer. Meteor. Soc.*, **63**, 29–43.

Betts, A. K., 1975: Parametric interpretation of trade-wind cumulus budget studies. *J. Atmos. Sci.*, **32**, 1934–1945.

Bunker, A. F., B. Haurwitz, J. S. Malkus and H. Stommel, 1949: Vertical distribution of temperature and humidity over the Caribbean Sea. Pap. Phy. Oceanogr. Meteor., II. No. 1, MIT and Woods Hole Inst., 82 pp.

Felde, G. W., 1983: The mean structure and eddy energetics of a central Pacific region during two periods in 1979. M.S. thesis, Dept. of Meteorology, Pennsylvania State University, 122 pp.

Ficker, H. von, 1936: Die passatinversion. *Veroff. Meteor. Inst. Berlin*, **1**, 33 pp.

Firestone, J. K., 1983: The structure and equatorward modification of the winter Pacific Ocean trades during FGGE. M.S. thesis, Dept. of Meteorology, The Pennsylvania State University, 138 pp.

Fitzjarrald, D. R., and M. Garstang, 1981: Vertical structure of the tropical boundary layer. *Mon. Wea. Rev.*, **108**, 1512–1526.

Fleming, R. J., T. M. Kareshige and W. E. McGovern, 1979a: The Global Weather Experiment, I. The observational phase through the first Special Observing Period. *Bull. Amer. Meteor. Soc.*, **55**, 649–659.

——, ——, —— and T. E. Bryan, 1979b: The Global Weather Experiment. II. The second Special Observing Period. *Bull. Amer. Meteor. Soc.*, **60**, 1316–1322.

Gaynor, J. E., and P. A. Mandics, 1978: An analysis of the tropical marine boundary layer during GATE. *Mon. Wea. Rev.*, **106**, 223–232.

——, and C. F. Ropelewski, 1979: Analysis of the convectively modified GATE boundary layer using in situ and acoustic sounder data. *Mon. Wea. Rev.*, **107**, 985–993.

Holland, J. S., and B. M. Rasmusson, 1973: Measurements of the atmospheric mass, energy and momentum budgets over a 500-kilometer square of tropical ocean. *Mon. Wea. Rev.*, **101**, 44–55.

Houze, R. A., Jr., 1977: Structure and dynamics of a tropical squall-line system observed during GATE. *Mon. Wea. Rev.*, **105**, 1540–1567.

——, and A. K. Betts, 1981: Convection in GATE. *Rev. Geophy. Space Phys.*, **19**, 541–576.

Johnson, R. H., 1981: Large-scale effects of deep convection on the GATE tropical boundary layer. *J. Atmos. Sci.*, **38**, 2399–2413.

——, and M. E. Nicholls, 1982: A composite analysis of the tropical boundary layer accompanying a tropical squall line. *Mon. Wea. Rev.*, **111**, 308–319.

Julian, P. R., 1982: The aircraft dropwindsonde system in the Global Weather Experiment. *Bull. Amer. Meteor. Soc.*, **63**, 619–627.

LeMone, M. A., and W. T. Pennell, 1976: The relationship of trade wind cumulus distribution to subcloud layer fluxes and structure. *Mon. Wea. Rev.*, **104**, 524–539.

Mahrt, L., 1976: Mixed layer moisture structure. *Mon. Wea. Rev.*, **104**, 1403–1407.

Malkus, J. S., 1978: On the structure of the trade wind moist layer. Pap. Phys. Oceanogr. and Meteor., XII, No. 2, MIT and Woods Hole Ocean Inst., 47 pp.

Neiburger, M., D. S. Johnson and C. W. Chein, 1961: Studies of the structure of the atmosphere over the eastern Pacific Ocean in summer, I. The inversion over the eastern north Pacific Ocean. *Univ. Calif. Publ. Meteor.*, **1**, 94 pp.

Newell, R. E., J. W. Kidson, D. G. Vincent and G. J. Boer, 1972: *The General Circulation of the Tropical Atmosphere and Interactions with Extratropical Latitudes, Vol. 1.* MIT Press, 258 pp.

Nicholls, S., and M. A. LeMone, 1980: The fair weather boundary layer in GATE: The relationship of subcloud fluxes and structure to the distribution and enhancement of cumulus clouds. *J. Atmos. Sci.*, **37**, 2051–2067.

——, and R. H. Johnson, 1984: A model of a tropical squall line boundary layer wake. *J. Atmos. Sci.*, **41**, 2774–2791.

Nitta, T., and S. Esbensen, 1974: Heat and moisture budgets using BOMEX data. *Mon. Wea. Rev.*, **102**, 17–28.

Ramage, C. S., S. J. S. Khalsa and B. N. Meisner, 1979: *The Central Pacific Near Equatorial Convergence Zone.* Dept. of Meteorology Rep. UHMET 79-11, University of Hawaii, 109 pp.

Reed, R. J., and E. E. Recker, 1971: Structure and properties of synoptic-scale wave disturbances in the equatorial western Pacific. *J. Atmos. Sci.*, **28**, 1117–1133.

Riehl, H., 1979: *Climate and Weather in the Tropics.* Academic Press, 611 pp.

——, T. C. Yeh, J. S. Malkus and N. E. LaSeur, 1951: The northeast trade of the Pacific Ocean. *Quart. J. Roy. Meteor. Soc.*, **77**, 598–626.

Schubert, W. H., 1976: Experiments with Lilly's cloud-topped mixed layer model. *J. Atmos. Sci.*, **33**, 436–446.

Smagorinsky, J., 1978: History and progress, U.S. Committee for the Global Atmospheric Research Program. *The Global Weather Experiment—Prospectives on Its Implementation and Exploitation,* National Academy of Sciences, Washington, DC, 104 pp.

Thompson, R. M., Jr., S. W. Payne, E. E. Recker and R. J. Reed, 1979: Structure and properties of synoptic-scale wave disturbances in the intertropical convergence zone of the eastern Atlantic. *J. Atmos. Sci.*, **36**, 53–72.

Wagner, A. J., 1979: Weather and circulation of January 1979. *Mon. Wea. Rev.*, **107**, 499–506.

Williams, K. T., and W. M. Gray, 1973: Statistical analysis of satellite observed trade wind cloud clusters in the western North Pacific. *Tellus*, **25**, 313–336.

Yanai, M., S. Esbensen and J. H. Chu, 1973: Determination of bulk properties of tropical cloud clusters from large-scale heat and moisture budgets. *J. Atmos. Sci.*, **30**, 611–627.

Zipser, E. J., 1969: The role of organized unsaturated convective downdrafts in the structure and rapid decay of an equatorial disturbance. *J. Appl. Meteor.*, **8**, 799–814.

——, 1977: Mesoscale and convective-scale downdrafts as distinct components of squall-line circulations. *Mon. Wea. Rev.*, **105**, 1568–1589.